Oncogene (2011) 30, 4864–4873

www.nature.com/onc

ORIGINAL ARTICLE

Pdcd4 directly binds the coding region of c-*myb* mRNA and suppresses its translation

P Singh[1], L Wedeken[1], LC Waters[2], MD Carr[2] and K-H Klempnauer[1]

[1]*Institute for Biochemistry, Westfälische-Wilhelms-Universität Münster, Münster, Germany and* [2]*Department of Biochemistry, University of Leicester, Leicester, UK*

Pdcd4 is a novel tumor suppressor protein that functions in the nucleus and the cytoplasm, and appears to be involved in the regulation of transcription and translation. In the cytoplasm, Pdcd4 has been implicated in the suppression of translation of mRNAs containing structured 5′-untranslated regions; however, the mechanisms that recruit Pdcd4 to specific target mRNAs and the identities of these mRNAs are mostly unknown. In this study, we have identified c-*myb* mRNA as the first natural translational target mRNA of Pdcd4. We have found that translational suppression of c-*myb* mRNA by Pdcd4 is dependent on sequences located within the c-*myb*-coding region. Furthermore, we have found that the N-terminal domain of Pdcd4 has an important role in targeting Pdcd4 to c-*myb* RNA by mediating preferential RNA binding to the Pdcd4-responsive region of c-*myb* mRNA. Overall, our work demonstrates for the first time that Pdcd4 is directly involved in translational suppression of a natural mRNA and provides the first evidence for a key role of the RNA-binding domain in targeting Pdcd4 to a specific mRNA.
Oncogene (2011) **30,** 4864–4873; doi:10.1038/onc.2011.202; published online 6 June 2011

Keywords: Pdcd4; c-*myb*; translation; RNA binding

Introduction

The programmed cell death 4 (*Pdcd4*) gene encodes a multi-functional nuclear–cytoplasmic shuttling protein that is involved in the regulation of transcription and translation and functions as a tumor suppressor (for recent review see Lankat-Buttgereit and Göke, 2009). Pdcd4 is highly conserved among vertebrates with homologs found also in distantly related species, such as *Drosophila melanogaster*, the sponge *Suberites domuncula* and even plants (http://pfam.sanger.ac.uk/). Pdcd4 contains two so-called MA-3 domains in the central and C-terminal parts of the protein, which mediate protein–protein interactions, and an N-terminal RNA-binding domain. *Pdcd4* was originally identified as a gene whose expression is increased during apoptosis (Shibahara *et al*., 1995), but has now been implicated as a tumor suppressor in a broad spectrum of human tumors. Pdcd4 was initially shown to suppress tumor development in an *in vitro* mouse keratinocyte model of tumor promotion (Cmarik *et al*., 1999). More recently, decreased expression of *Pdcd4* has been implicated in the development and progression of human lung, colon, liver and breast cancer (Chen *et al*, 2003; Afonja *et al*, 2004; Zhang *et al*., 2006; Mudduluru *et al*., 2007). Pdcd4 expression is controlled by multiple mechanisms. *Pdcd4* mRNA is targeted by microRNA miR-21, whose overexpression in cancer cells downregulates *Pdcd4* expression (Asangani *et al*., 2008; Lu *et al*., 2008). On the protein level, p70(S6K) kinase-mediated phosphorylation of Pdcd4 triggers its ubiquitinylation by the E3 ubiquitin ligase complex SCF(betaTRCP) and its subsequent degradation (Dorello *et al*., 2006). Recent work has suggested that downregulation of Pdcd4 expression contributes to tumor development by stimulating the mobility and metastatic potential of tumor cells (Leupold *et al*., 2007; Asangani *et al*., 2008), and by deregulating the cellular DNA damage response (Bitomsky *et al*., 2008; Singh *et al*., 2009).

Pdcd4 has emerged as an important regulator of both transcription and translation. Pdcd4 affects transcription of certain genes by modulating the activities of specific transcription factors, such as c-Jun (Yang *et al*., 2003b; Bitomsky *et al*., 2004), Sp1 (Leupold *et al*., 2007) and p53 (Bitomsky *et al*., 2008). As a translation regulator, Pdcd4 interacts with the eukaryotic translation initiation factor eIF4A, a RNA helicase that catalyzes the unwinding of mRNA secondary structures in 5′-untranslated regions (UTRs) (Yang *et al*., 2003a, 2004). Binding of Pdcd4 to eIF4A is mediated by the MA-3 domains, whose structure and complex formation with eIF4A have been analyzed in detail (LaRonde-LeBlanc *et al*., 2007; Waters *et al*., 2007, 2011; Suzuki *et al*., 2008; Chang *et al*., 2009; Loh *et al*., 2009). Because binding of Pdcd4 to eIF4A inhibits the helicase activity of eIF4A (Yang *et al*., 2003a; Yang *et al*, 2004), it is believed that Pdcd4 functions as a suppressor of cap-dependent translation of mRNAs with structured 5′-UTRs. This assumption was supported by studies, which assessed the effects of Pdcd4 on the translation of

Correspondence: Dr K-H Klempnauer, Institute for Biochemistry, Westfälische-Wilhelms-Universität Münster, Wilhelm-Klemm-Strasse 2, Münster D-48149, Germany.
E-mail: klempna@uni-muenster.de
Received 22 December 2010; revised 14 April 2011; accepted 27 April 2011; published online 6 June 2011

artificial RNAs containing 5′-hairpin structures (Yang *et al*., 2003a, 2004); however, because physiological translational target mRNAs for Pdcd4 have not yet been unambiguously identified, it is presently unclear whether translation of all RNAs containing structured 5′-UTRs are suppressed by Pdcd4 or whether there are mechanisms that allow Pdcd4 to target specific mRNAs.

In this study, we report the identification of proto-oncogene c-*myb* mRNA as the first physiological target RNA of Pdcd4. We show that Pdcd4 is associated with c-*myb* mRNA and suppresses its translation. The inhibitory effect of Pdcd4 is mediated by sequences located within the c-*myb*-coding region. We demonstrate that the Pdcd4 RNA-binding domain has a key role in targeting Pdcd4 to c-*myb* mRNA by mediating preferential binding of Pdcd4 to RNA secondary structure formed by the response region in c-*myb* mRNA. In summary, our work demonstrates for the first time that Pdcd4 is directly involved in translational suppression of a natural mRNA and offers the first insight into how Pdcd4 targets a specific mRNA.

Results

c-myb *mRNA is a translational target of Pdcd4*

We have previously shown that Pdcd4 inhibits the activity of transcription factors c-Jun and p53 by interfering with their ability to cooperate with p300 (Bitomsky *et al*., 2004, 2008). While studying the effect of Pdcd4 on c-Myb, another transcription factor recruiting p300, we noted that Pdcd4 strongly decreased the amount of c-Myb generated from a cytomegalovirus (CMV) promoter-based c-Myb expression vector. The inhibitory activity of Pdcd4 was specific, because the amounts of β-galactosidase, C/EBPβ or green fluorescent protein (GFP) derived from similar CMV promoter-based expression vectors were not affected. The inhibitory activity was shared by avian and human Pdcd4 (Figure 1a), and was also observed when expression vectors for mouse or human c-Myb were used (data not shown), indicating that it was a conserved feature of Pdcd4 and c-Myb. The reduced expression of c-Myb was not accompanied by lower steady-state levels

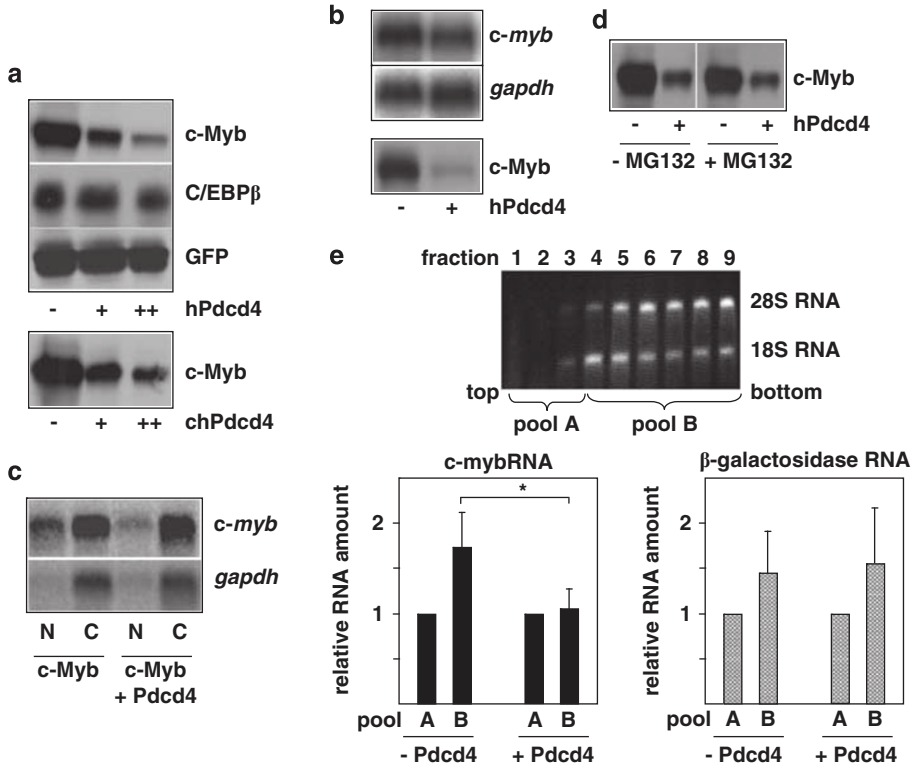

Figure 1 Pdcd4 suppresses translation of c-*myb* mRNA. (**a**) QT6 fibroblasts were transfected with plasmids encoding chicken c-Myb (2 μg), chicken C/EBPβ (2 μg), EGFP (2 μg) and human or chicken Pdcd4 (2 and 5 μg). Total protein extracts were analyzed by western blotting with antibodies against c-Myb, C/EBPβ or GFP. (**b**) Cells were transfected with expression vectors for c-Myb and human Pdcd4. Polyadenylated RNA was analyzed by northern blotting using *myb* and *gapdh* probes (top) or by western blotting for the expression of c-Myb (bottom). (**c**) QT6 cells transfected as in (**b**) were fractionated into nuclear (N) and cytoplasmic (C) fractions, and RNA isolated from both fractions was analyzed by northern blotting using *myb* and *gapdh* probes. (**d**) QT6 cells transfected as in (**b**) were treated with 10 μM MG132 for 5 h or were left untreated. Cells were analyzed by western blotting as in (**b**). (**e**) QT6 cells were transfected as in (**a**). Cytoplasmic extracts were sedimented through 10–50 % sucrose density gradients. Aliquots of the gradient fractions were analyzed by agarose gel electrophoresis for the distribution of ribosomal RNAs (top). Subsequently, fractions 1–3 and 4–9 were pooled as non-ribosomal (pool A) and ribosomal fractions (pool B), respectively. RNA isolated from these fractions was then analyzed by quantitative real-time PCR for c-*myb* (black columns) and β-galactosidase (gray columns) mRNAs. The columns show the amounts of both RNAs in the ribosomal compared with the non-ribosomal fractions. The amounts present in the non-ribosomal factions were normalized to 1. The asterisk indicates statistical significance ($P<0.005$; Student's-*t* test).

or altered nuclear–cytoplasmic distribution of *myb* mRNA (Figures 1b and c), suggesting that Pdcd4 neither affected the transcription or the stability of c-*myb* mRNA nor its nuclear export. Furthermore, blocking protein degradation by the proteasome inhibitor MG132 did not abolish the inhibitory effect of Pdcd4. This indicated that Pdcd4 did not decrease the amount of c-Myb by stimulating its degradation (Figure 1d). Taken together, these experiments suggested that Pdcd4 suppresses the translation of c-Myb. To substantiate this conclusion we subjected cytoplasmic extracts of cells transfected with c-Myb or c-Myb plus Pdcd4 expression vectors to sucrose density gradient centrifugation. We then analyzed the distribution of c-*myb* mRNA between non-ribosome-containing fractions and mono- or polyribosome-containing fractions. This allowed us to determine whether Pdcd4 affected the amount of c-*myb* RNA engaged in translation (i.e., associated with ribosomes). Figure 1e shows that the amount of ribosome-associated c-*myb* RNA was decreased when Pdcd4 was expressed, consistent with the notion that Pdcd4 inhibits the translation of c-*myb* mRNA. The Pdcd4-dependent decrease of ribosomal association of c-*myb* RNA was specific, as the distribution of β-galactosidase mRNA, used as internal control, was not affected by Pdcd4.

To assess the effect of Pdcd4 on c-Myb expression under more physiological conditions we made use of a Pdcd4-deficient clone of the chicken DT40 cell line that we had established previously (Singh *et al*., 2009). Consistent with the results of Figure 1, the steady-state level of c-Myb was increased in the Pdcd4 knockout cells (Figure 2a). Northern blotting showed that this increase was not due to increased transcription of c-*myb* (Figure 2b). Treatment of the cells with the proteasome inhibitor MG132 did not abolish the difference of the amount of c-Myb between wild-type and Pdcd4-deficient cells, indicating that this difference was not due to different half-lives of c-Myb in both cells (Figure 2c). Furthermore, we compared the turnover of c-Myb in the DT40 wildtype and Pdcd4 knockout cells after blocking protein synthesis with cycloheximide to confirm that there was no significant difference in the half-life of the protein in both cells (Figure 2d). To confirm that the increased expression of c-Myb was caused by the loss of Pdcd4, we re-expressed chicken Pdcd4 in the knockout cells. Figure 2e shows that restoration of Pdcd4 expression reduced the amount of c-Myb in the knockout cells to the level found in wild-type DT40 cells. Taken together, the experiments illustrated in Figures 1 and 2 provide strong evidence that c-*myb* mRNA is a translational target of Pdcd4. This conclusion was further supported by demonstrating that Pdcd4 also inhibits translation of c-Myb in an *in vitro* translation system (Supplementary Figure S1).

We have previously shown that transcription of *Pdcd4* is stimulated by v-Myb and c-Myb (Schlichter *et al*., 2001a, b; Appl and Klempnauer, 2002). The finding that translation of c-*myb* mRNA is suppressed by Pdcd4 suggests that the expression of both genes is controlled

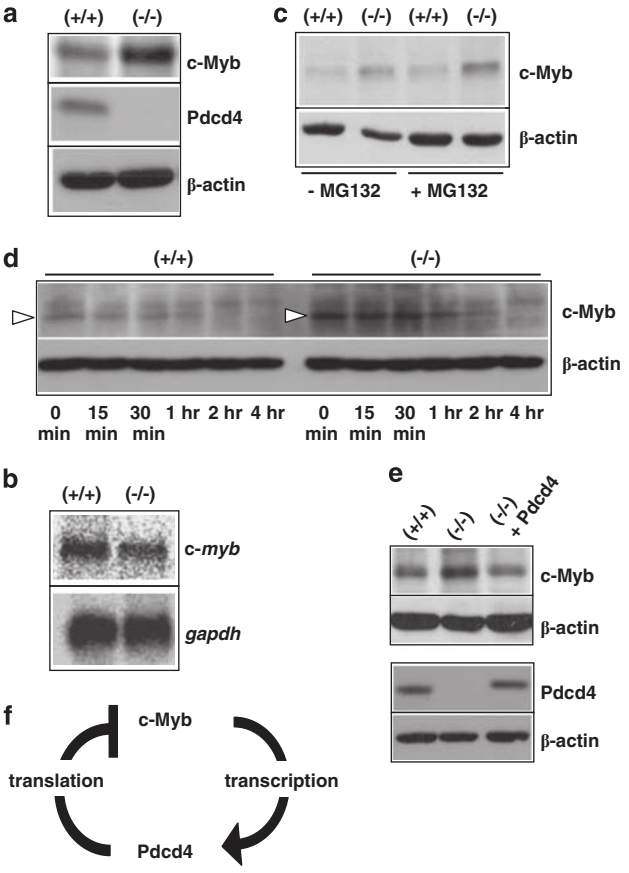

Figure 2 Analysis of c-Myb expression in wildtype and Pdcd4-deficient DT40 cells. (**a**) Wild-type DT40 (+/+) and *Pdcd4* knockout (−/−) cells were analyzed by western blotting for expression of c-Myb (top), Pdcd4 (middle) and β-actin (bottom). (**b**) mRNA from wild-type DT40 (+/+) and *Pdcd4* knockout (−/−) cells was analyzed by northern blotting for expression of c-*myb* and *gapdh* mRNAs. (**c**) Extracts from wild-type DT40 (+/+) and *Pdcd4* knockout (−/−) cells were analyzed by western blotting as in (**a**). Cells were treated with 10 μM of MG132 for 5 h or left untreated. (**d**) Wild-type DT40 (+/+) and *Pdcd4* knockout (−/−) cells were treated with 50 μg/ml cycloheximide. The cells were harvested after the indicated time periods and analyzed by western blotting for the expression of c-Myb (top) and β-actin (bottom). The bands corresponding to c-Myb are marked by white arrowheads. (**e**) Wild-type DT40 (+/+), *Pdcd4* knockout (−/−) and knockout cells re-expressing Pdcd4 were analyzed by western blotting for expression of c-Myb and β-actin (top) and Pdcd4 and β-actin (bottom). The re-expressed Pdcd4 contains a hemagglutinin tag, explaining its slightly larger size. (**f**) Schematic illustration of an autoregulatory feedback loop established by c-Myb and Pdcd4.

by an autoregulatory feedback loop, as illustrated in Figure 2f.

Pdcd4 is associated with c-myb *mRNA* in vivo

To investigate whether c-*myb* mRNA is a direct translational target of Pdcd4 we asked whether Pdcd4 is associated with c-*myb* mRNA *in vivo*. To address this question we transfected fibroblasts with combinations of expression vectors for c-Myb, luciferase and Pdcd4, followed by analysis of cytoplasmic extracts by RNA immunoprecipitation (RIP). The cells were treated with formaldehyde to crosslink protein–RNA complexes, and cytoplasmic extracts were then immunoprecipitated

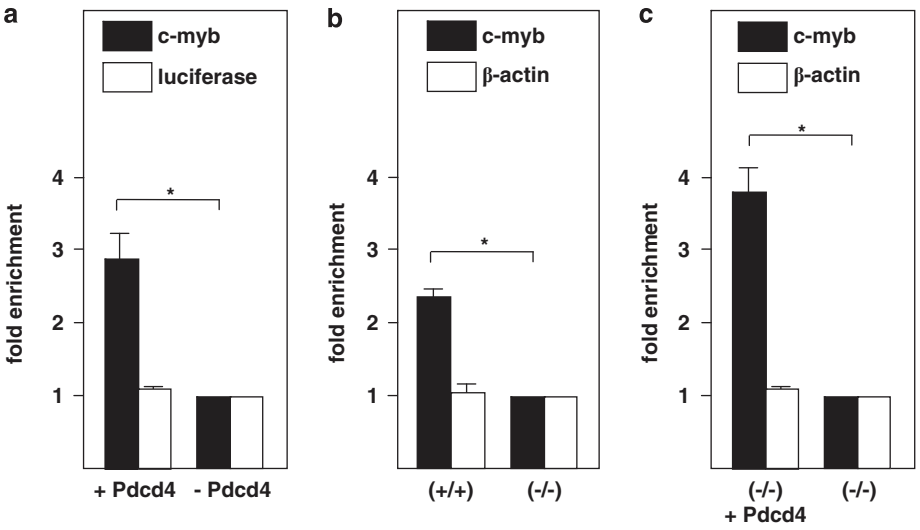

Figure 3 Pdcd4 is associated with c-*myb* mRNA *in vivo*. (**a**) QT6 fibroblasts were transfected with plasmids encoding chicken c-Myb (2 μg), luciferase (0.5 μg) and human Pdcd4 (5 μg), as indicated. Cytoplasmic extracts were subjected to RIP with Pdcd4-specific antibodies. Columns show the relative amounts of c-*myb* (black bars) and luciferase (white bars) RNAs in the immunoprecipitates, as determined by quantitative real-time PCR. The amounts of *myb* and luciferase RNAs present in control precipitate (i.e., from cells transfected only with c-Myb and luciferase expression plasmids) were normalized to 1. (**b**) DT40 (+/+) and *Pdcd4* (−/−) cells were subjected to RIP using Pdcd4-specific antibodies. The amounts of c-*myb* (black columns) and β-actin (white columns) RNAs present in the immunoprecipitates were quantified by real-time PCR. The amounts of both RNAs present in a control precipitate derived from the (−/−) cells were normalized to 1. (**c**) DT40 *Pdcd4* (−/−) cells and Pdcd4 (−/−) cells re-expressing Pdcd4 were analyzed by RIP as in (**b**). The asterisks indicate statistical significance ($P<0.005$; Student's *t*-test).

with antibodies against Pdcd4, followed by reverse transcription of the co-precipitated RNA and PCR analysis. As shown in Figure 3a, c-myb RNA was enriched in the immunoprecipitate derived from Pdcd4 expressing cells. This enrichment was specific because it was not observed when the Pdcd4 expression vector was omitted and because luciferase RNA, which was used as an internal control, was not enriched. This experiment, therefore, demonstrated that Pdcd4 is associated with c-*myb* RNA *in vivo*. To confirm the binding of Pdcd4 to c-*myb* mRNA under physiological conditions we also analyzed DT40 cells by RIP. Figure 3b shows that c-*myb* RNA was enriched by IP from extracts from DT40 wildtype cells but not from extracts from Pdcd4-deficient cells. This enrichment was specific, as β-actin mRNA, which was analyzed as an internal control, was not enriched. Finally, Pdcd4-deficient cells reconstituted with the Pdcd4 expression vector again showed specific enrichment of c-*myb* mRNA in a RIP experiment (Figure 3c). Taken together, these experiments clearly demonstrated that Pdcd4 is associated with c-*myb* mRNA *in vivo*.

The c-myb-*coding region contains a translational 'Pdcd4-response element'*

The finding that c-*myb* RNA is physically associated with Pdcd4 permitted us to investigate how Pdcd4 targets a specific mRNA. Because Pdcd4 suppressed translation of *myb* RNA transcribed from a CMV promoter-based expression vector containing only the c-*myb*-coding region, this suggested that the sequences responsible for targeting Pdcd4 to c-*myb* RNA are located in the coding region of the mRNA. To identify the part of the c-*myb* mRNA that mediates the inhibitory effect of Pdcd4, we first generated 3′-deletions of the c-Myb expression vector and examined the effect of Pdcd4 on the steady-state levels of the resulting truncated proteins. As illustrated in Figure 4b, truncation of 3′ of the coding region up to a *Bgl*II or a *Sal*I site, leading to the expression of truncated c-Myb proteins containing amino acids 1–497 and 1–303, respectively, did not significantly affect the ability of Pdcd4 to inhibit translation. When the deletion of coding sequences was extended to a *Nae*I site, translation of the resulting protein (amino acids 1–236) was no longer suppressed by Pdcd4. We therefore concluded that the translational 'Pdcd4-response element' maps to 5′-sequences to the *Sal*I site. We also performed RIP experiments using extracts from cells transfected with expression vectors from full-length and truncated c-Myb. These experiments showed that the RNA encoding the truncated c-Myb protein, which was no longer suppressed by Pdcd4 (c-Myb ΔNae), was also not associated with Pdcd4 *in vivo* (Figure 4d).

To map the Pdcd4-responsive region from the 5′-end of c-*myb* mRNA, we analyzed N-terminal deletion mutants of c-Myb (Figure 4c). These experiments showed that c-*myb*-coding sequences between the 5′-end and an *Xma*I site could be deleted without abrogating the inhibitory effect of Pdcd4. Together with the data illustrated in Figure 4b this showed that the 'Pdcd4-response region' maps to the center of the c-*myb*-coding region between the *Xma*I and *Sal*I sites.

Pdcd4 has been shown to suppress cap-dependent initiation of translation by interacting with eIF4A and inhibiting its helicase activity (Yang *et al*., 2003a, 2004);

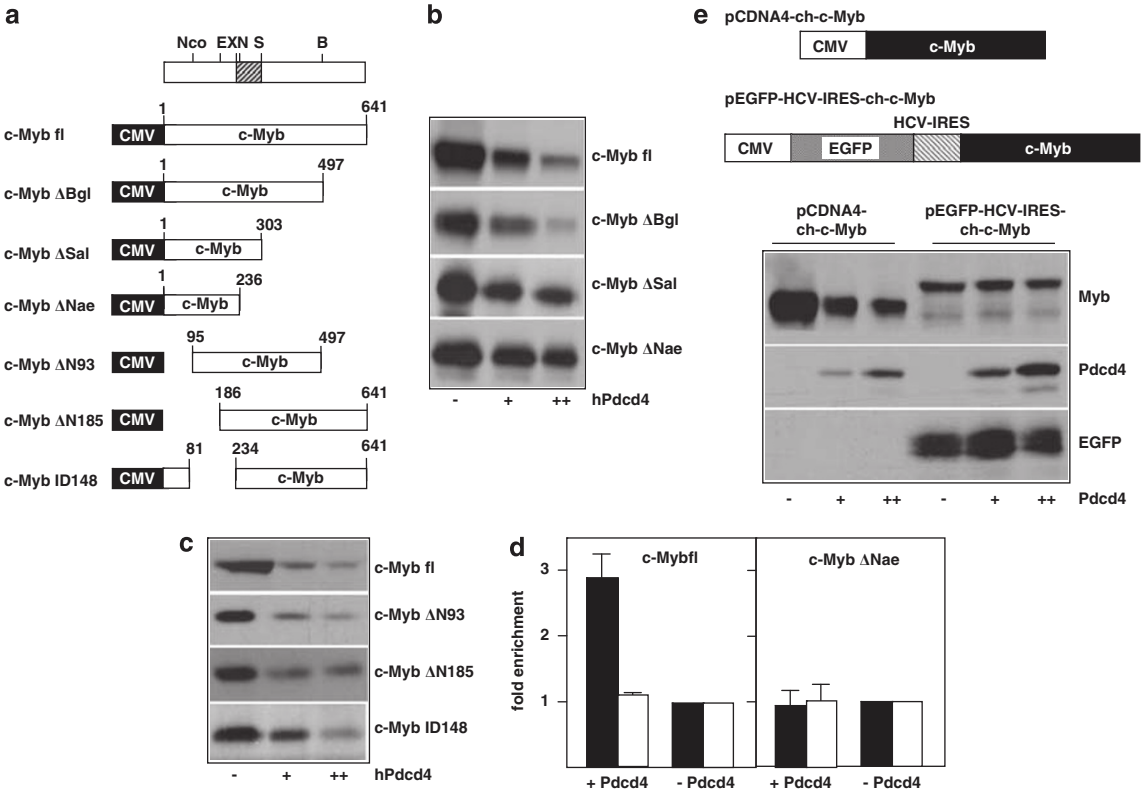

Figure 4 Suppression of translation by Pdcd4 is mediated by sequences in the center of the c-*myb*-coding region. (**a**) Schematic illustration of c-Myb deletion constructs. Numbers refer to amino acids. Nco, E, X, N, S and B refer to restriction sites for *Nco*I, *Eco*RI, *Xma*I, *Nae*I, *Sal*I and *Bgl*II, respectively. The hatched region marks the Pdcd4 target region. (**b**, **c**) QT6 fibroblasts were transfected with plasmids encoding full-length or truncated versions of c-Myb (2 μg each) and Pdcd4 (2 and 5 μg), as well as with the β-galactosidase expression vector pCMVβ (0.5 μg). Cells were harvested after 24 h and the β-galactosidase activity was determined. β-galactosidase-normalized amounts of cell extracts were then analyzed by western blotting with antibodies against c-Myb. (**d**) QT6 cells were transfected with plasmids encoding full-length or ΔNae-truncated c-Myb, Pdcd4 and firefly luciferase. Cytoplasmic extracts were subjected to RIP with Pdcd4-specific antibodies. The amounts of c-*myb* (black columns) and luciferase (white columns) mRNAs present in the immunoprecipitates were determined by quantitative real-time PCR. The amounts of *myb* and luciferase RNAs present in control precipitate (i.e., from cells transfected without Pdcd4 expression vector) were normalized to 1. (**e**) QT6 fibroblasts were transfected with the mono- and bicistronic c-Myb expression vectors shown at the top, with or without increasing amounts (2 and 5 μg) of Pdcd4 expression vector. Cell extracts were analyzed by western blotting with antibodies against c-Myb, Pdcd4 or GFP. c-Myb encoded by the bicistronic expression vector has a slightly higher molecular weight because translation is started within the hepatitis C virus internal ribosomal entry site.

however, because the Pdcd4-responsive region is located within the coding region of c-*myb* mRNA, we also considered the possibility that Pdcd4 might function by slowing down elongating ribosomes or causing ribosomal drop-off. Ribosomal drop-off has been implicated in the translational inhibition caused by microRNAs that target the coding region of certain mRNAs (Nottrott *et al*., 2006; Petersen *et al*., 2006). To explore this possibility we constructed a bicistronic expression vector in which the c-*myb*-coding region is placed downstream of the hepatitis C virus internal ribosomal entry site. If Pdcd4 functions by inhibiting ribosomal elongation, c-Myb expression will still be suppressed by Pdcd4 under these conditions. On the other hand, if Pdcd4 suppresses cap-dependent initiation of translation, c-Myb expression might not be affected because the mechanism of translational initiation at the hepatitis C virus internal ribosomal entry site is distinct from cap-dependent translation initiation and does not require translation initiation factors (Lancaster *et al*., 2006). Figure 4e clearly shows that Pdcd4 failed to suppress the expression of c-Myb when its translation was initiated at the hepatitis C virus internal ribosomal entry site, indicating Pdcd4 does not inhibit elongating ribosomes.

*The Pdcd4 N-terminal domain is required for suppression of c-*myb *translation and binds preferentially to the Pdcd4-response region of c-*myb *mRNA.*

To understand how Pdcd4 is recruited to c-*myb* mRNA we investigated the role of the Pdcd4 N-terminal domain in translational suppression of c-*myb* RNA. Previous work has shown that the amino terminal domain of Pdcd4 binds to RNA and that its RNA-binding activity is mediated by two clusters of basic amino acids. Mutation of both clusters (which are referred to as RBM1 and 2) results in a complete loss of the RNA-binding activity (Böhm *et al*., 2003; Wedeken *et al*., 2010). As shown in Figure 5, mutant Pdcd4 carrying mutations of the basic amino acid clusters inhibited c-Myb translation less strongly than wild-type Pdcd4,

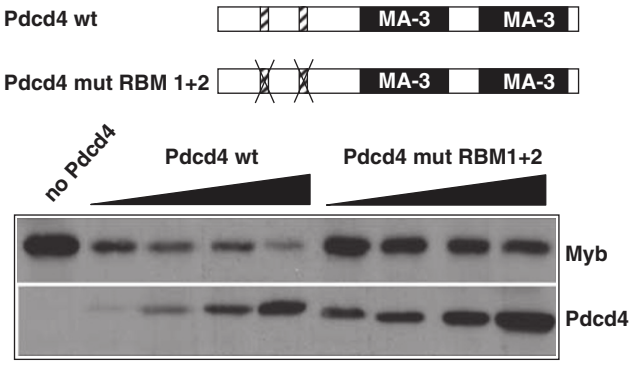

Figure 5 Disruption of the RNA-binding domain reduces the suppressive activity of Pdcd4. The RNA-binding-deficient mutant Pdcd4-mutRBM1 + 2 is shown schematically at the top. QT6 fibroblasts were transfected with plasmids encoding full-length c-Myb (2 μg) and increasing amounts of the indicated Pdcd4 expression vectors. Total protein extracts were analyzed by western blotting with antibodies against c-Myb and Pdcd4.

indicating that RNA binding is required for efficient translational suppression of c-*myb* mRNA. This suggested that Pdcd4 might target *myb* RNA by a direct protein–RNA interaction with the 'Pdcd4-response element' in the c-*myb*-coding region.

To explore this possibility and to substantiate a role of RNA binding in targeting Pdcd4 to c-*myb* mRNA we prepared GST–Pdcd4 fusion proteins having the wild-type or a mutated RNA-binding domain, and performed RNA electrophoretic mobility shift assays with *in vitro* synthesized RNAs. As shown in Figure 6a, we generated three overlapping RNAs from the central part of the c-*myb* mRNA (referred to as c-myb#1, 2 and 3). Upon electrophoresis in native polyacrylamide gels, each of the RNAs gave rise to fast- and slow-migrating forms, the latter of which disappeared upon heat denaturation (Figure 6b). This indicated that the slower migrating forms are due to the formation of secondary structures. The propensity to form secondary structure was most prominent in case of RNA c-myb#3, which corresponds to the central part of the Pdcd4-response region. We performed RNA secondary structure prediction by M-fold (http://mfold.bioinfo.rpi.edu) to confirm that RNA c-myb#3 is indeed able to form a significant amount of secondary structure (Supplementary Figure S2). Figure 6d shows that wild-type Pdcd4 bound preferentially to the slower migrating form of RNA c-myb#3, as is evident from the fact that the slow-migrating form of the RNA was efficiently shifted to even slower migrating complexes appearing in the upper part of the gel, whereas the fast-migrating form of the RNA, which lacks secondary structure, remained virtually unbound by Pdcd4, under these conditions. The mutant Pdcd4, used as negative control, did not bind to any of the RNA forms. The RNA bound by Pdcd4 appeared as a continuous smear in the upper part of the gel, suggesting that Pdcd4 does not form stable protein–RNA complexes under the conditions of electrophoresis. To substantiate our conclusion that Pdcd4 binds preferentially to the structured form of the RNA, we also performed additional RNA-binding experiments in which we used unlabeled c-myb#3 RNA as competitor (Figure 6e). Overall, these experiments confirmed that the structured form of the RNA was much more effective as a competitor when the denatured form of the RNA was used as the radiolabeled probe rather than the native form (compare lanes 3–5 and 8–10 of Figure 6e). Furthermore, the denatured form of unlabeled c-myb#3 RNA competed less well than the native form of this RNA (compare lanes 8–10 and 11–13 of Figure 6e). We also compared the binding of Pdcd4 to RNA c-myb#3 and an unrelated RNA (c-myb1-111) derived from the 5′-end of c-*myb* mRNA, which is not involved in Pdcd4-dependent suppression of c-Myb translation (Figure 6f). This RNA also formed secondary structure, as evidenced by the appearance of fast- and slow-migrating bands and the disappearance of the slow-migrating form after heat denaturation (Figure 6g). Interestingly, binding of Pdcd4 to the structured form of c-myb#3 was more efficient than binding to the structured form of the RNA from the 5′-end of c-Myb, indicating that preferential binding of Pdcd4 is mediated by a specific RNA structural motif formed by the Pdcd4-response region of c-*myb* mRNA, and not by the formation of secondary structure *per se*. We also compared the binding of Pdcd4 to the denatured forms of RNAs c-myb#3 and c-myb1-111. As shown in Figure 6g, there was no significant difference in binding to both denatured RNAs. Taken together, these experiments provide the first evidence that the Pdcd4 RNA-binding domain has an intrinsic preference for binding to an RNA structural motif. The fact that such a motif is formed by that part of c-*myb* mRNA that is essential for translational suppression of the RNA by Pdcd4 strongly suggests that Pdcd4 is recruited to c-*myb* mRNA, at least in part, by preferential RNA binding.

Discussion

In this work, we have identified chicken c-*myb* mRNA as the first physiological and direct translational target of Pdcd4. The amount of c-Myb protein generated from a transfected c-Myb expression vector is significantly decreased by Pdcd4. We have shown that this decrease is not due to decreased transcription, altered nuclear export of the mRNA or effects of Pdcd4 on c-Myb protein stability. Rather, we have demonstrated that the association of c-*myb* mRNA with ribosomes is decreased by Pdcd4. Importantly, by using Pdcd4 knockout cells, we have confirmed that Pdcd4 affects c-*myb* mRNA translation also in non-transfected cells not overexpressing Pdcd4. Finally, we have demonstrated that Pdcd4 is physically associated with c-*myb* mRNA *in vivo*. Altogether, these data provide compelling evidence that c-*myb* mRNA is a direct translational target of Pdcd4.

We have previously shown that c-Myb directly activates transcription of the *Pdcd4* gene via an array of Myb binding sites in the promoter of the *Pdcd4* gene (Schlichter *et al*., 2001a, b, Appl and Klempnauer, 2002). The finding that Pdcd4 suppresses the translation

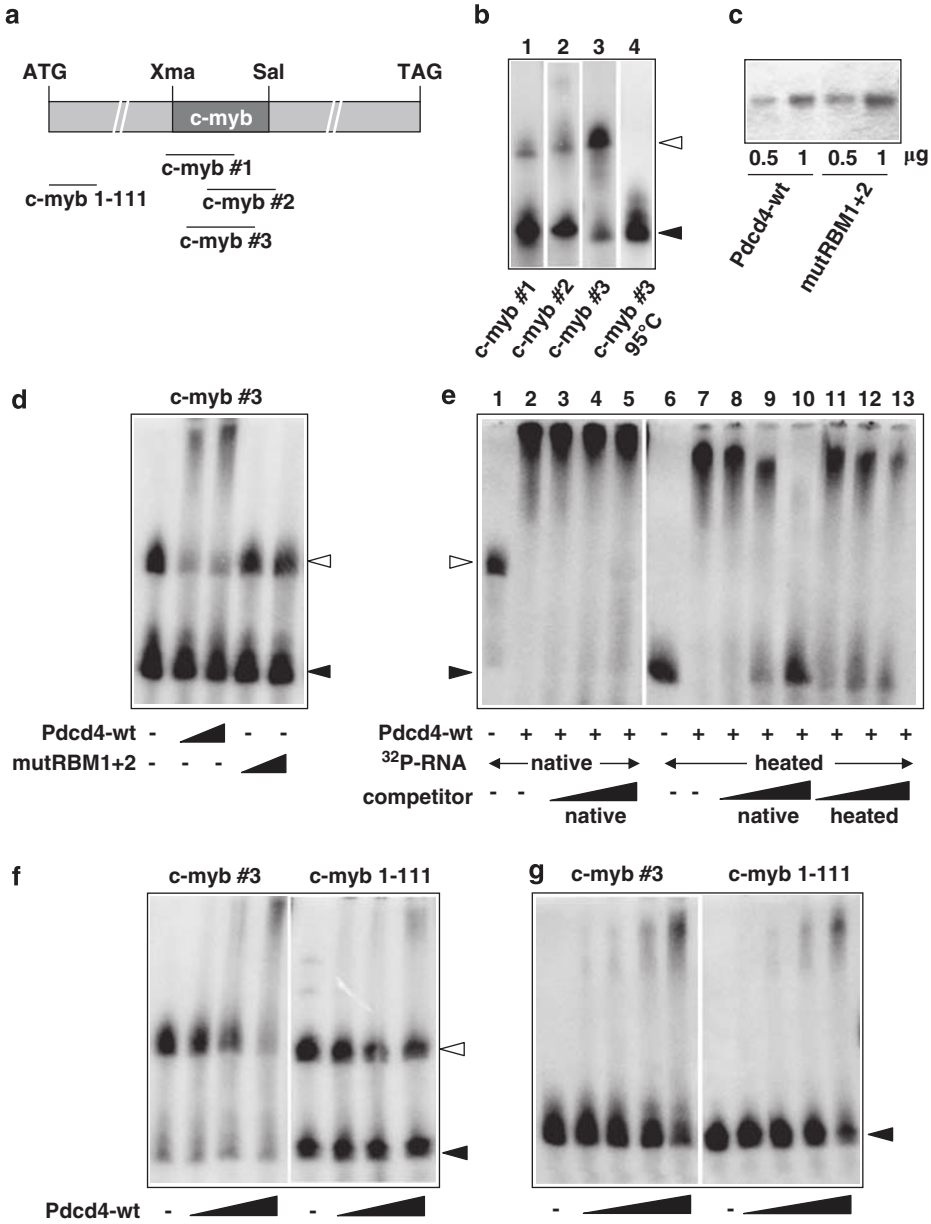

Figure 6 *In vitro* RNA binding of Pdcd4 to the Pdcd4-response region of c-*myb* mRNA. (**a**) *In vitro* transcribed RNAs from different parts of c-*myb* are shown schematically. The Pdcd4-response region (located between the *Xma*I and *Sal*I sites) is highlighted. (**b**) *In vitro* transcribed c-myb #1, #2 and #3 RNAs were analyzed by gel electrophoresis without (lanes 1–3) or after (lane 4) heat denaturation. Black and white arrowheads mark fast- and slow-migrating forms of the RNAs. (**c**) Purified GST-Pdcd4-wt and GST-Pdcd4-mutRBM1 + 2 were analyzed by SDS–PAGE and stained with Coomassie brilliant blue. (**d**) A mixture of the RNAs shown in lanes 3 and 4 of panel (**b**) was subjected to an electrophoretic mobility shift assay with increasing amounts (0.25 and 0.5 µg) of the indicated GST-Pdcd4 proteins. (**e**) Competition binding experiments using different combinations of native or heat-denatured c-myb#3 RNA as radiolabeled probe or as unlabeled competitor RNA. The same amount of wild-type GST-Pdcd4 protein (0.5 µg) was used in binding reactions. (**f**) RNA binding assays of native c-myb #3 and c-myb 1–111 RNAs incubated with or without increasing amounts (0.0625, 0.125 and 0.25 µg) of wild-type GST-Pdcd4. (**g**) RNA binding assays of heat-denatured c-myb #3 and c-myb 1–111 RNAs incubated with or without increasing amounts (0.0625, 0.125, 0,25 and 0.5 µg) of wild-type GST-Pdcd4.

of c-*myb* mRNA places c-Myb and Pdcd4 in a regulatory feedback loop in which Pdcd4 restricts c-Myb activity by suppressing its synthesis. Such a feedback mechanism might be important to control the proliferation-stimulating activity of c-Myb and would be consistent with Pdcd4's function as a tumor suppressor. This might be relevant, for example, in colon cancer in which downregulation of Pdcd4 expression and increased c-*myb* expression are frequently associated with highly malignant states (Mudduluru *et al*., 2007; Ramsay and Gonda, 2008).

The identification of c-*myb* mRNA as a target of Pdcd4 has allowed, for the first time, to examine how Pdcd4 is targeted to a specific mRNA. Our data indicate

that Pdcd4 targets a 'Pdcd4-response element' that maps to the coding region of c-*myb* mRNA. At first glance, it appears unusual that the coding region of an mRNA is the target of a translational regulatory mechanism; however, genome-wide analyses of interactions of regulatory RNA-binding proteins with mRNAs have revealed surprisingly large numbers of interactions that take place in the coding regions of the cognate mRNAs (Hogan *et al*., 2008; Hafner *et al*., 2010). Previous studies have also identified specific regulatory proteins that bind to the coding regions of certain mRNAs, such as the thymidylate synthase and dihydrofolate reductase, both of which bind to the coding regions of their own mRNAs (Ercikan-Abali *et al*., 1997; Lin *et al*., 2000; Zhang *et al*., 2010) and the RNA-binding protein HuR, which interacts with the coding region of CD83 RNA (Prechtel *et al*., 2006). Target sites for microRNAs are also not restricted to the 3′-UTRs but can occur in the coding region of certain mRNAs. Such target sites are clearly functional as they have been shown to mediate translational suppression of the respective mRNAs (Nottrott *et al*., 2006; Petersen *et al*., 2006).

Our analysis of the binding of Pdcd4 to c-*myb* RNA also highlights the role of the Pdcd4 N-terminal domain whose physiological function has not been clarified so far. Initially, *in vitro* binding experiments using non-specific RNA suggested that the N-terminal part of Pdcd4 is involved in RNA binding (Böhm *et al*., 2003). More recently, we have shown that the Pdcd4 RNA-binding domain is required for the association of Pdcd4 with ribosomal complexes *in vivo*, providing the first evidence for a role of RNA binding in targeting Pdcd4 to the translation machinery (Wedeken *et al*., 2010). The identification of a 'Pdcd4-response region' in c-*myb* mRNA has allowed, for the first time, to study RNA binding of Pdcd4 in the context of a physiological RNA target site. As a result, our work provides the first evidence that the Pdcd4 RNA-binding domain is able to preferentially recognize specific RNA regions and suggests that RNA binding by Pdcd4 has a key role in targeting of Pdcd4 to specific mRNAs. Interestingly, it appears that not a RNA sequence *per se* is recognized by Pdcd4 but rather a secondary structure formed by the RNA is recognized.

Overall, our work demonstrates for the first time that Pdcd4 is directly involved in translational suppression of a natural mRNA and offers a framework for how Pdcd4 targets specific mRNAs. It will now be interesting to identify and characterize additional Pdcd4 target mRNAs to further explore this mechanism.

Materials and methods

Cells and transfections

Transient transfections were performed in the QT6 fibroblast line as described (Bitomsky *et al*., 2008). To monitor and normalize transfection efficiencies, the β-galactosidase expression plasmid CMVβ (Invitrogen, Karlsruhe, Germany) was included in each transfection. DT40 Pdcd4 (−/−) cells and Pdcd4 (−/−) cells re-expressing hemagglutinin-tagged versions of Pdcd4 have been described (Singh *et al*., 2009).

Expression vectors

The chicken c-Myb expression vector was obtained by isolating the coding region of full-length c-Myb as a *Nco*I (partial)/*Xba*I fragment from pCM100 plasmid (Foos *et al*., 1992) and inserting it together with an oligonucleotide adapter (GAATTCACCATGG) between the *Eco*RI and *Xba*I sites of pCDNA4 (Invitrogen). pCDNA4-chcmyb-ΔBgl, pCDNA4-chcmyb-ΔSal and pCDNA4-chcmyb-ΔNae are derivatives encoding C-terminally truncated proteins containing c-*myb* amino acids 1–497, 1–303 and 1–236, respectively. pCDNA4-chcmyb-ΔN93, pCDNA4-chcmyb-ΔN185 and pCDNA4-chcmyb-ID148 encode N-terminally truncated proteins lacking amino acids 2–95, 2–186 and 81–234, respectively. The bicistronic GFP-HCV-Myb expression vector was generated by first inserting the hepatitis C virus internal ribosomal entry site and the c-*myb*-coding region into pEGFP-C1 (Clontech, Heidelberg, Germany) downstream of the GFP-coding region. In the resulting plasmid, the HCV translational start codon is linked via a 123 base-pair sequence in-frame to the c-Myb start codon. pCDNA4-CCR encodes full-length chicken C/EBPβ (Plachetka *et al*, 2008). pCMVluc was obtained by inserting the CMV promoter into pGL3-basic (Promega, Mannheim, Germany). Expression vectors for hemagglutinin-tagged chicken Pdcd4 and wild-type human Pdcd4 have been described (Schlichter *et al*., 2001a; Waters *et al*., 2007) pCDNA4-hPdcd4-mutRBM1 + 2 encodes a mutant Pdcd4 protein with amino-acid substitutions of several basic amino acids in the N-terminal part of Pdcd4 (Wedeken *et al*., 2010). Bacterial expression vectors for GST-Pdcd4 and GST-Pdcd4 mutRBM1 + 2 have been described (Wedeken *et al*., 2010).

Antibodies

Western blotting of chicken and human c-Myb was performed with Myb-specific monoclonal antibodies 5E11 (Sleeman, 1993) and myb 2–37 (Evan *et al*., 1984). C/EBPβ was detected with a rabbit antiserum raised against full-length chicken C/EBPβ (Mink *et al*., 1996). Pdcd4 was detected with a rabbit antiserum raised against the N-terminus of human Pdcd4 (Bitomsky *et al*., 2008) or with a commercial antibody against the C-terminus of Pdcd4 (Upstate Biomol, Hamburg, Germany). Antibodies against GFP were obtained from Roche Diagnostics (Mannheim, Germany).

Nuclear/cytoplasmic fractionation

Cells were lysed in hypotonic buffer (10 mM Hepes, pH 7.5; 5 mM KCl; 2 mM $MgCl_2$; 0.5% NP40; 1 mM phenylmethanesulfonylfluoride supplemented with with RNase inhibitor RNaseOUT (Invitrogen) and a protease inhibitor cocktail of pepstatin A, leupeptin hemisulfate and aprotinin) and pelleted at 10 000 r.p.m. for 10 min at 4° C. RNA prepared from the supernatant (cytoplasmic fraction) and the pellet (nuclear fraction) was analyzed by northern blotting as described (Bitomsky *et al*., 2008).

Sucrose density gradients

Density gradient centrifugation was performed as described (Wedeken *et al*., 2010). Ribosomal RNAs were visualized by agarose gel electrophoresis. For real-time PCR analysis, gradient fractions were treated with proteinase K, and RNA was isolated by ribozol-OLS (Omni Life Sciences, Hamburg, Germany) extraction and ethanol precipitation. cDNA synthesis and real-time PCR were performed as described for RIP.

RNA immunoprecipitation

Approximately 6×10^5 QT6 cells or 10^8 DT40 cells were fixed with 0.5% formaldehyde in growth medium for 10 min at

room temperature, followed by addition of 125 mM glycine for 5 min. Cells were lysed in hypotonic buffer. Approximately 10% of the supernatant (cytoplasmic fraction) was saved as input sample and the remainder was used for IP for 12 h at 4 °C, using a commercial Pdcd4 antiserum (Upstate), in case of DT40 cells, or rabbit antiserum raised against the N-terminus of human Pdcd4 (Bitomsky *et al*., 2008), in case of transiently transfected cells. Immunoprecipitates were collected on protein-A sepharose for 2 h at 4 °C and washed several times with RIPA buffer (10 mM Hepes, pH 7.5; 50 mM NaCl; 0.5% NP40; 0.1% SDS; 0.5% sodium deoxycholate; 1 mM phenylmethanesulfonylfluoride; supplemented with protease cocktail and RNase inhibitor). After elution from the beads with 1% SDS, samples were reverse crosslinked for 4 h at 65 °C and further treated with RNase-free DNase I for 15 min at 37° C, followed by proteinase K treatment for 1 h at 42° C. RNA was purified by ribozol-OLS (Omni Life Sciences) extraction and ethanol precipitation. First-strand cDNA synthesis was performed with a cDNA kit (Fermentas, St. Leon Roth, Germany). The cDNAs were analyzed by quantitative real-time PCR using the following primer pairs: c-*myb*: 5′-CCA TGGACTAAAGAGGAGGATCA-3′ and 5′-CCTCTCCCT GCACTGTTTTCC-3′, β-actin: 5′-ATGGCTCCGGTATGT GCAA-3′ and 5′-TGTCTTTCTGGCCCATACCAA-3′, β-galactosidase: 5′-CTGGCTGGAGTGCGATCTTC-3′ and 5′-GGCGGATTGACCGTAATGG-3′, luciferase: 5′-TTTGT GCCAGAGTCCTTCGAT-3′ and 5′-GAGAATCTCACGC AGGCAGTT-3′.

Electrophoretic mobility shift assay

Subregions from the central part of the c-*myb* corresponding to nucleotides 660–822 (c-myb #1), 740–949 (c-myb #2) and 714–880 (c-myb #3) of the coding region were amplified by PCR using primers with flanking *Hin*dIII and *Bam*HI sites and cloned into the polylinker of pCDNA3. RNAs were transcribed from *Bam*HI-digested template DNA in a volume of 20 µl, using 1 µg template DNA, 1 × T7 buffer (Invitrogen), 40 U/ml RNaseOUT (Invitrogen), 4 mM rNTPs, 8 mM $MgCl_2$, 25 µCi α^{32}P-UTP (3000 Ci/mmol) and 50 U T7 RNA polymerase (Invitrogen) for 1 h at 37 °C. An additional RNA (c-myb 1–111) corresponding to nucleotides 1–111 of the c-*myb*-coding region was transcribed from pCDNA3-chc-myb (containing the full-length c-*myb*-coding region) and digested with *Avr*II. The RNA was extracted with TriZOL, ethanol-precipitated and dissolved in diethylpyrocarbonate-treated water. GST-Pdcd4-wt and GST-Pdcd4-mutRBM1 + 2 have been described (Wedeken *et al*., 2010). The proteins were purified by binding to GST sepharose in buffer containing 1 × phosphate-buffered saline, 1% NP-40, 2 mM DTT, 1 mM phenylmethanesulfonylfluoride and a protease inhibitor cocktail containing pepstatin A, leupeptin and aprotinin. To remove bacterial nucleic acids bound to the protein, the beads were then washed twice with binding buffer containing 300 mM NaCl and 150 mM KCl. Finally, after washing twice with 10 mM Tris–HCl, pH 7.5, the bound protein was eluted in 10 mM Tris–HCl, pH 7.5, supplemented with 15 mM reduced glutathione. The final concentration of GST-Pdcd4 was determined by SDS–PAGE, using known amounts of bovine serum albumin as standard. RNA-binding reactions were set up in 20 µl volume and contained approximately 4×10^6 c.p.m. radioactive RNA, 5 mM Tris–HCl, pH 7.5; 50 mM NaCl, 1 mM EDTA, 2% w/v ficoll and different amounts of bacterially expressed protein. Binding reactions were incubated for 30 min on ice and analyzed by electrophoresis in 5% polyacrylamide (0.5 × TBE) gels. Gels were dried and analyzed with a phosphor image analyzer (Fuji film, Duesseldorf, Germany).

Conflict of interest

The authors declare no conflict of interest.

Acknowledgements

We thank M Hentze and D Ostareck for providing plasmids. This work was supported by the Deutsche Krebshilfe (10–1716), the Wilhelm-Sander-Stiftung (2004.088.1) and the Wellcome Trust. PS and LW were supported by the Graduate School of Chemistry (GSC-MS) at the University of Münster.

References

Afonja O, Juste D, Das S, Matsuhashi S, Samuels HH. (2004). Induction of PDCD4 tumor suppressor gene expression by RAR agonists, antiestrogen and HER-2/neu antagonist in breast cancer cells. Evidence for a role in apoptosis. *Oncogene* **23**: 8135–8145.

Asangani IA, Rasheed SA, Nikolova DA, Leupold JH, Colburn NH, Post S *et al*. (2008). MicroRNA-21 (miR-21) post-transcriptionally downregulates tumor suppressor Pdcd4 and stimulates invasion, intravasation and metastasis in colorectal cancer. *Oncogene* **27**: 2128–2136.

Appl H, Klempnauer K-H. (2002). Targeted disruption of c-*myb* in the chicken pre B-cell line DT40. *Oncogene* **21**: 3076–3081.

Bitomsky N, Böhm M, Klempnauer K-H. (2004). Transformation suppressor protein Pdcd4 interferes with JNK-mediated phosphorylation of c-Jun and recruitment of the coactivator p300 by c-Jun. *Oncogene* **23**: 7484–7493.

Bitomsky N, Wethkamp N, Marikkannu R, Klempnauer K-H. (2008). siRNA-mediated knock-down of Pdcd4 expression causes up-regulation of p21(Waf1/Cip1) expression. *Oncogene* **27**: 4820–4829.

Böhm M, Sawicka K, Siebrasse JP, Brehmer-Fastnacht A, Peters R, Klempnauer K-H. (2003). The transformation suppressor protein Pdcd4 shuttles between nucleus and cytoplasm and binds RNA. *Oncogene* **22**: 4905–4910.

Chang JH, Cho YH, Sohn SY, Choi JM, Kim A, Kim YC *et al*. (2009). Crystal structure of the eIF4A-PDCD4 complex. *Proc Natl Acad Sci USA* **106**: 3148–3153.

Chen Y, Knosel T, Kristiansen G, Pietas A, Garber ME, Matsuhashi S *et al*. (2003). Loss of PDCD4 expression in human lung cancer correlates with tumour progression and prognosis. *J Pathol* **200**: 640–646.

Cmarik JL, Min H, Hegamyer G, Zhan S, Kulesz-Martin M, Yoshinaga H *et al*. (1999). Differentially expressed protein Pdcd4 inhibits tumor promoter-induced neoplastic transformation. *Proc Natl Acad Sci USA* **96**: 14037–14042.

Dorello NV, Peschiamoli A, Guardavaccaro D, Colburn NH, Sherman NE, Pagano M. (2006). S6K1- and betaTRCP-mediated degradation of PDCD4 promotes protein translation and cell growth. *Science* **314**: 467–471.

Ercikan-Abali EA, Banerjee D, Waltham MC, Skacel N, Scotto KW, Bertino JR. (1997). Dihydrofolate reductase protein inhibits its own translation by binding to dihydrofolate reductase mRNA sequences within the coding region. *Biochemistry* **36**: 12317–12322.

Evan GI, Lewis GK, Bishop JM. (1984). Isolation of monoclonal antibodies specic for products of avian oncogene *myb*. *Mol Cell Biol* **4**: 2843–2850.

Foos G, Grimm S, Klempnauer K-H. (1992). Functional antagonism between members of the *myb* family: B-*myb* inhibits v-*myb* induced gene activation. *EMBO J* **11**: 4619–4629.

Hafner M, Landthaler M, Burger L, Khorshid M, Hausser J, Berninger P *et al*. (2010). Transcriptome-wide identification of RNA-binding protein and microRNA target sites by PAR-CLIP. *Cell* **141**: 129–141.

Hogan DJ, Riordan DP, Gerber AP, Herschlag D, Brown PO. (2008). Diverse RNA-binding proteins interact with functionally related sets of RNAs, suggesting an extensive regulatory system. *PLos Biol* **6**: e255.

Lancaster AM, Jan E, Sarnow P. (2006). Initiation factor-independent translation mediated by the hepatitis C virus internal ribosomal entry site. *RNA* **12**: 894–902.

Lankat-Buttgereit B, Göke R. (2009). The tumor suppressor Pdcd4: recent advances in the elucidation of function and regulation. *Biol Cell* **101**: 309–317.

LaRonde-LeBlanc N, Santhanam AN, Baker AR, Wlodawer A, Colburn NH. (2007). Structural basis for inhibition of translation by the tumor suppressor Pdcd4. *Mol Cell Biol* **27**: 147–156.

Leupold JH, Yang HS, Colburn NH, Asangani I, Post S, Allgayer H. (2007). Tumor suppressor Pdcd4 inhibits invasion/intravasation and regulates urokinase receptor (u-PAR) gene expression via Sp-transcription factors. *Oncogene* **26**: 4550–4562.

Lin X, Parsels LA, Voeller DM, Allegra CJ, Maley GF, Maley F *et al*. (2000). Characterization of a *cis*-acting regulatory element in the protein coding region of thymidylate synthase mRNA. *Nucleic Acids Res* **28**: 1381–1389.

Loh PG, Yang HS, Walsh MA, Wang Q, Wang X, Cheng Z *et al*. (2009). Structural basis for translational inhibition by the tumour suppressor Pdcd4. *EMBO J* **28**: 274–285.

Lu Z, Liu M, Stribinskis V, Klinge CM, Ramos KS, Colburn NH. (2008). MicroRNA-21 promotes cell transformation by targeting the programmed cell death 4 gene. *Oncogene* **27**: 4373–4379.

Mink S, Kerber U, Klempnauer K-H. (1996). Interaction of C/EBPβ and v-Myb is required for synergistic activation of the *mim-1* gene. *Mol Cell Biol* **16**: 1316–1325.

Mudduluru G, Medved F, Grobholz R, Jost C, Gruber A, Leupold JH *et al*. (2007). Loss of programmed cell death 4 expression marks adenoma-carcinoma transition, correlates inversely with phosphorylated protein kinase B, and is an independent prognostic factor in resected colorectal cancer. *Cancer* **110**: 1697–1707.

Nottrott S, Simard MJ, Richter JD. (2006). Human let-7a miRNA blocks protein production on actively translating polyribosomes. *Nat Struct Mol Biol* **13**: 1108–1114.

Petersen CP, Bordeleau M-E, Pelletier J, Sharp PA. (2006). Short RNAs repress translation after initiation in mammalian cells. *Mol Cell* **21**: 533–542.

Plachetka A, Chayka O, Wilczek C, Melnik S, Bonifer C, Klempnauer K-H. (2008). C/EBPβ induces chromatin opening at a cell-type-specific enhancer. *Mol Cell Biol* **28**: 2102–2112.

Prechtel AT, Chemnitz J, Schirmer S, Ehlers C, Langbein-Detsch I, Stülke J *et al*. (2006). Expression of CD83 is regulated by HuR via a novel *cis*-active coding region element. *J Biol Chem* **281**: 10912–10925.

Ramsay RG, Gonda TJ. (2008). Myb function in normal and cancer cells. *Nat Rev Cancer* **8**: 523–534.

Schlichter U, Burk O, Worpenberg S, Klempnauer K-H. (2001a). The chicken Pdcd4 gene is regulated by v-Myb. *Oncogene* **20**: 231–239.

Schlichter U, Kattmann D, Appl H, Miethe J, Brehmer-Fastnacht A, Klempnauer K-H. (2001b). Identification of the *myb*-inducible promoter of the chicken Pdcd4 gene. *Biochim Biophys Acta* **1520**: 99–104.

Shibahara K, Asano M, Ishida Y, Aoki T, Koike T, Honjo T.. (1995). Isolation of a novel mouse gene MA-3 that is induced upon programmed cell death. *Gene* **166**: 297–301.

Singh P, Marikkannu R, Bitomsky N, Klempnauer K-H. (2009). Disruption of the Pdcd4 tumor suppressor gene in chicken DT40 cells reveals its role in the DNA-damage response. *Oncogene* **28**: 3758–3764.

Sleeman JP. (1993). Xenopus A-*myb* is expressed during early spermatogenesis. *Oncogene* **8**: 1931–1941.

Suzuki C, Garces RG, Edmonds KA, Hiller S, Hyberts SG, Marintchev A *et al*. (2008). PDCD4 inhibits translation initiation by binding to eIF4A using both its MA3 domains. *Proc Natl Acad Sci USA* **105**: 3274–3279.

Waters LC, Strong SL, Ferlemann E, Oka O, Muskett FW, Veverka V *et al*. (2011). Structure of the tandem MA-3 region of Pdcd4 and characterization of its interactions with eIF4A and eIF4G: molecular mechanisms of a tumour suppressor. *J Biol Chem* **285**: 17270–17280.

Waters LC, Veverka V, Böhm M, Schmedt T, Choong PT, Muskett FW *et al*. (2007). Structure of the C-terminal MA-3 domain of the tumour suppressor protein Pdcd4 and characterization of its interaction with eIF4A. *Oncogene* **26**: 4941–4950.

Wedeken L, Ohnheiser J, Hirschi B, Wethkamp N, Klempnauer K-H. (2010). Association of tumor suppressor protein Pdcd4 with ribosomes is mediated by protein-protein and protein-RNA interactions. *Genes Cancer* **1**: 293–301.

Yang HS, Cho MH, Zacowicz H, Hegamyer G, Sonenberg N, Colburn N. (2004). A novel function of the MA-3 domains in transformation and translation suppressor Pdcd4 is essential for its binding to eukaryotic translation initiation factor 4A. *Mol Cell Biol* **24**: 3894–3906.

Yang HS, Jansen AP, Komar AA, Zheng X, Merrick WC, Costes S *et al*. (2003a). The transformation suppressor Pdcd4 is a novel eukaryotic translation initiation factor 4A binding protein that inhibits translation. *Mol Cell Biol* **23**: 26–37.

Yang HS, Knies JL, Stark C, Colburn NH. (2003b). Pdcd4 suppresses tumor phenotype in JB6 cells by inhibiting AP-1 transactivation. *Oncogene* **22**: 3712–3720.

Zhang H, Ozaki I, Mizuta T, Hamajima H, Yasutake T, Eguchi Y *et al*. (2006). Involvement of programmed cell death 4 in transforming growth factor-beta1-induced apoptosis in human hepatocellular carcinoma. *Oncogene* **25**: 6101–6112.

Zhang Y, Yang S, Liu M, Song C, Wu N, Ling P *et al*. (2010). Interaction between thymidylate synthase and its cognate mRNA in zebrafish embryos. *PLos One* **5**: e10618.

Supplementary Information accompanies the paper on the Oncogene website (http://www.nature.com/onc)